ABSTRACT

All stars in the Galaxy form from interstellar clouds composed primarily of molecular hydrogen. These clouds are, in turn, surrounded by significant concentrations of atomic hydrogen. It is thought that molecular clouds form out of the larger, atomic hydrogen concentrations. By studying the relationship between the gas and dust in these clouds, we hope to gain a fuller understanding of how they form and evolve. In order to achieve this, a 4 degree by 2 degree region centered on the interstellar molecular cloud, MBM40, was mapped in the 21 cm spectral line of atomic hydrogen with the 305-meter radio telescope at the Arecibo Observatory in Puerto Rico. A data cube with axes consisting of right ascension (celestial longitude), declination (celestial latitude) and velocity (Doppler shift of the spectral line) was produced from the raw data. Presented within the thesis is the atomic hydrogen data in a series of velocity "snapshots". These elucidate the relationship between the atomic structures enveloping the cloud and both the carbon monoxide spectral data (which traces the molecular component of the cloud) and the infrared data from the IRAS satellite (which traces the dust component in the region). Our results show that there is a positional offset between the molecular and atomic gas. It is likely that this offset reflects the transition to molecular gas of a portion of a larger pre-existing, atomic hydrogen cloud. Thus, these results indicate that MBM 40 is condensing out of a larger scale flow and is structured by shear flow turbulence.

THE ATOMIC HYDROGEN ENVIRONMENT OF MBM 40

By

MEREDITH NEAL MCCARTHY

A Thesis Submitted to the Honors Council of the University of Georgia in Partial Fulfillment of the Requirements for the Degree

BACHELOR OF SCIENCE

and

HONORS IN PHYSICS

Athens, Georgia

2003

THE ATOMIC HYDROGEN ENVIRONMENT OF MBM 40

By

MEREDITH NEAL MCCARTHY

Approved:

Dr. Loris Magnani — 05/07/2003
Date

Major Professor

Approved:

Dr. F. Scott Shaw — 05/07/2003
Date

Reader

Approved:

Jere W. Morehead — 05/07/2003
Date

Associate Provost and Director,
Honors Program

DEDICATION

To Dr. Loris Magnani, who knows I am better at sarcasm than sincerity. From the heart, thank you for your patience, knowledge, friendship, and humor.

ACKNOWLEDGEMENTS

First and foremost I would like to thank my boyfriend Kevin Foster for his love, care, and amazing Photoshop skills. Thank you for your great sacrifices and faith in our future.

From the Physics and Astronomy Department I wish to again acknowledge the work of Dr. Loris Magnani, and to thank Dr. J. Scott Shaw for graciously reading this thesis.

Thanks to Phil Perillat of Arecibo Observatory for his assistance in the data reduction, and Snezana Stanimirovic of the University of California, Berkley for her datacube routine. Thanks to the staff scientists and telescope operators at Arecibo.

Thanks to my mother, Mary Sullivan McCarthy, for instilling in me the drive to succeed and a thirst for knowledge. And finally thanks to my father, Michael McCarthy, who gave me strength and patience.

TABLE OF CONTENTS

FIGURES

TABLES

Chapter 1 – High Latitude Molecular Clouds and the Galaxy

Our galaxy, the Milky Way (referred to hereafter as "the Galaxy"), is comprised primarily of stars and interstellar medium, which is simply dust particles and atomic and molecular gas distributed between the stars. The gas is more abundant than the dust, as far as mass is concerned, by roughly a factor of 100 (Spitzer 1978). However, both gas and dust (and also magnetic fields) play a key role in the formation of stars. Understanding the relationship and interplay between gas, dust, and stars is fundamental to understanding the structure and evolution of the Galaxy and comprises the basic mission of Galactic astronomy.[1]

This study focuses primarily on one aspect of the interstellar medium, the gas, and even more specifically, the gas composing one particular cloud-like structure in the Galaxy. Thus, it is necessary to explain the merits of studying such an object, and how this understanding contributes to our further understanding of the Galaxy as a whole. To do this, we first examine the relationship between the basic components of the galaxy, and then delve deeper into the significance of one specific component, the molecular clouds.

[1] Astronomy can be broadly divided into four areas: planetary astronomy which studies the Sun, planets, the Solar system and other solar-like systems; galactic and stellar astronomy, described above; extragalactic astronomy which studies the distribution, evolution, and properties of galaxies outside the Milky Way; and cosmology, the study of the Universe as a whole.

1.1 The Star-Gas Cycle

Stars are created from concentrations of primarily molecular gas and dust called molecular clouds. They are discrete entities with well-defined boundaries. However, they have nothing to do with terrestrial water vapor clouds; their name comes from their ragged morphology, somewhat reminiscent of the shapes seen in terrestrial clouds. At the end of their evolutionary cycle, stars return much (more than 70%) of their material to the atomic interstellar medium. The relationship between stars and the interstellar medium is called the Star-Gas Cycle, and can be summarized by Figure 1.1.

The cycle can be thought to begin with the cold atomic hydrogen portion of the interstellar medium (hereafter called H I).[2] H I is neutral, and lies predominately in the galactic plane. H I cools and combines to form molecular hydrogen (H_2), which then clumps and forms the entities known as molecular clouds. Molecular clouds are important because these are the regions which form new stars. Protostars (collapsing spheres of primarily molecular gas and atomic helium, which are heating up by the conversion of gravitational potential energy into kinetic and then thermal energy) form in the densest gas and dust regions of molecular clouds. They then evolve into main sequence stars when thermonuclear fusion of H into He stabilizes the newly-formed star. These main sequence stars are of two general types, low mass and high mass stars. Low mass stars return atomic gas to the interstellar medium by stellar "winds"[3] during their lifetime and by planetary nebulae at their deaths. High mass stars return atomic gas to the interstellar medium by even stronger stellar winds, and, once they become red giants, they return molecules and dust at prodigious rates. When their fuel supply finally runs

[2] There are also warm (~8000 K) and hot (~10^6 K) phases of atomic hydrogen but they do not concern the subject of this thesis.
[3] Stellar winds are high-speed discharges of charged particles, probably driven by magnetic fields.

out, high mass stars spew most of the material in their outer layers into the interstellar medium by means of violent supernova explosions. However, not all material is returned to the interstellar medium. The cores of low mass stars become white dwarfs, and the cores of high mass stars become either neutron stars or black holes. One can think of white dwarfs, neutron stars, and black holes as being the "waste products" of the cycle. The Star-Gas cycle neatly describes the processes at work in a typical spiral galaxy. Galactic astronomers can spend their entire careers on one or more aspect of the cycle.

The focus of this study is on the portion of the cycle involving the interstellar medium; in particular, the relationship between the H I and molecular regions of a molecular cloud. There are several different theories to explain what causes H I to form molecular clouds. To determine which is correct, a better understanding of molecular clouds and the atomic environment around them is necessary.

1.2 Overview of Molecular Gas Clouds

Molecular clouds are the sites of all Galactic star formation (Blitz 1978). Their gaseous composition is basically H_2 and atomic helium. However, the H_2 molecule is extremely difficult to detect from the ground, thus rarer, more easily detected molecules are observed and hydrogen and helium concentrations are then extrapolated from these trace species. For example, carbon dioxide (CO) has its lowest rotational transition (from the first excited rotational state, J = 1, to the ground state, J = 0) at a wavelength of 2.6 mm and is the most commonly used tracer for H_2. The ratio between CO and H_2 (known as the abundance of CO) is on average 10^{-4} for most molecular clouds. Thus, surveys of the CO (J = 1-0) transition at 2.6 mm are effectively surveys of cold H_2. The CO (J = 1-0)

transition was first detected in the interstellar medium by Wilson et al. (1970) and, throughout the 1970's, surveys of CO emission along the Galactic plane were conducted by several groups (Stark 1979; Burton & Gordon 1978; Dame 1984; Sanders, Soloman, & Scoville 1984). These surveys quickly identified large concentrations of molecular gas which came to be known as Giant Molecular Clouds.

Giant Molecular Clouds are the most common regions of star formation, and are among the largest structures in the galaxy. They are characterized by masses between 10^3 and 10^6 solar masses and dimensions between 15 and 100 parsecs.[4] Giant Molecular Clouds are found within the Galactic plane, and are not uniform in density. Dense, gravitationally bound clumps within the clouds are prolific star forming regions, and virtually all high and low mass stars form in these nurseries of cold gas and dust. The general distribution of Giant Molecular Clouds can be seen in the H_2 map of the galaxy, shown in Figure 1.2.

Smaller, lower density, and lower mass clouds (solar masses less than 10^3) also lie throughout the Galactic plane. This type of molecular cloud usually contains high density gravitationally bound cores which tend to form low mass stars. However, the smaller molecular clouds also encompass types of objects which sometimes do not form stars. Van Dishoeck and Black (1988) divided the small molecular clouds into three groups determined by their absorption of background starlight (the absorption is produced by the dust contained within them) and their chemistry. The three types of small molecular clouds are known as dark, translucent, and diffuse, depending upon how opaque they are to optical light. The opacity of a cloud to optical light is often expressed in terms of a quantity known as visual extinction, A_v. The quantity A_v is

[4] 1 solar mass is $2x10^{30}$ kg and 1 parsec is $3.1x10^{18}$ cm.

approximately linear with the optical depth, τ, where τ is defined by the equation $I = I_o e^{-\tau}$ where I is the intensity of light the observer sees, I_o is the intensity of light before it enters the cloud, and τ is the optical depth. Objects with $\tau < 1$ can be considered transparent while those with $\tau > 3$ or 4 can be considered opaque. Because τ is linear with A_v, the three types of small molecular clouds can be classified according to their visual extinction. Diffuse clouds have $A_v < 1$, translucent clouds have $1 \leq A_v < 5$, and dark clouds have $A_v > 5$ (van Dishoeck & Black 1988).

Diffuse clouds have low molecular abundances; most of the gas is in atomic form, so the molecular component is difficult to detect. The easiest way to detect molecular lines in these clouds is to look for optical or ultraviolet spectral absorption lines against the continuous radiation field of a background star, as shown in Figure 1.3. The amount of gas in these types of clouds is very low, so that radio detection of molecular lines is either difficult or impossible. Thus, studies of these optically thin clouds can only be done along the infinitesimally small solid angle subtended by the star. Because their visual extinction is typically $A_v < 1$ magnitude, ultraviolet photons from the stellar radiation field permeate the clouds, and so their chemistry is driven by photochemical processes.

Dark clouds are named for their high levels of visual extinction produced by their high concentrations of dust. Visual extinction in these clouds can be significantly greater than 5 magnitudes in the most opaque regions. Dark clouds have been studied and cataloged extensively by Barnard (1927) and Lynds (1962), and molecules were quickly identified in virtually all dark clouds by radio spectroscopic techniques. Dark clouds lie primarily in the Galactic plane, have their chemistry driven by collisional processes, and can be regions of low mass star formation. Because dark clouds are so opaque that

background stars cannot be seen through them, they are studied primarily by radio spectroscopic techniques.

In between the dark and diffuse regimes are translucent clouds, with a mixture of dark and diffuse cloud properties. Their visual extinctions are 1 magnitude $\leq A_v < 5$ magnitudes, and they can be studied both through radio and optical spectroscopy. Their chemistry is driven both by photoprocesses and collisional processes. The majority of translucent clouds which have been found to date are at high Galactic latitudes ($|b| \geq 25^\circ$; see Appendix A) and were identified by Magnani, Blitz, and Mundy (1985). The specific cloud which will be discussed in this thesis is a translucent cloud, so their properties will be discussed in more detail below.

1.3 Properties of Translucent Clouds

Translucent molecular clouds tend to be small structures of 10-100 solar masses. They can be found isolated from other molecular clouds or they can be situated in groups. Most of the so-called high latitude molecular clouds are translucent in nature (Magnani, Hartmann & Speck 1996). Most translucent clouds do not appear to be gravitationally bound – that is, their internal motions can overcome the gravity between their molecular components (called the self-gravity of the cloud). If gravity does not hold them together, it is likely that these clouds are breaking up. In other words, they are transient objects with lifetimes ~ 106 years (Magnani, Blitz, & Mundy 1985). This is very different from the Giant Molecular Clouds which are bound and probably long-lived. It is not clear whether translucent clouds are capable of forming stars. The ones at the low-extinction end of the translucent range (i.e. $1 \leq A_v < 2$ magnitudes) almost surely cannot form stars

(Hearty 1998); whether the ones with extinctions closer to that of dark clouds ($A_v \sim 5$ magnitudes) form stars or not is still and open question. The cloud selected for this study, MBM 40 (see Chapter 2) does not have star formation present within its confines (Hearty 1998). The last important characteristic of translucent clouds is that many of them are very close to the Sun (~100 pc). They are the nearest molecular clouds, and so studies of their basic properties can be carried out at the greatest resolution.

1.4 H I and High Latitude Molecular Clouds

With a basic understanding of molecular clouds, the connection between H I and cloud formation in the Star-Gas Cycle can be further examined. H I is the most prevalent component of the interstellar medium, and is concentrated in the Galactic plane. Figure 1.4 is a composite image of H I observations of the Milky Way in the 21 cm emission line. Compared to Figure 1.2, it is easy to see the correspondence between H I and H_2 distributions; molecular clouds tend to form in regions containing high densities of H I. However, it is virtually impossible to determine any specifics about the relationship between the atomic and molecular hydrogen from this low resolution data. Additionally, the column density[5] of the H I in the Galactic plane is so great that it obscures any individual features or structures that might be the atomic component of a molecular cloud. There is simply too much H I in the Galactic plane down any line of sight, and it is difficult to match H I emission to H_2 emission because of all the H I in the foreground and in the background.

[5] Column density is the total number of particles of a given species in a "tube" of area $1cm^{-2}$ extending all along the line of sight.

In order to understand this crucial stage in the Star-Gas Cycle better, the Galactic plane should be avoided. Referring again to Figure 1.4, H I is additionally found in regions above and below the Galactic plane. These are called high latitude regions (see Appendix A). Common H I structures are filamentary and located along the edges of larger pockets of hot gas, resulting in shapes such as arcs, loops, and shells. Gir, Blitz, and Magnani (1994) have shown that the population known as high latitude molecular clouds form in these regions. The high latitude molecular clouds are for the most part translucent clouds, and are located at galactic latitudes $|b| \geq 25^{\circ}$.[6] These clouds are ideal targets for studying the relationship between H I and H_2, because at this high latitude, the confusion due to large quantities of H I along the galactic plane is significantly reduced. At high latitudes the structural composition of a molecular cloud and its associated atomic hydrogen can be more easily unraveled.

To understand high latitude molecular clouds, it is necessary to understand the structures that form them – the filamentary arcs, loops and shells of H I. Two basic theories have been presented; high latitude molecular clouds are formed from shocks that compress the gas until it becomes molecular, or shear flows cause thermal instabilities, which create cooler pockets of H I that then combine to form H_2. This issue is one of the driving questions of this study and is discussed in Chapter 5. By comparing the H I morphology of a translucent high latitude molecular cloud to its molecular structure, it is hoped that a conclusive picture of the formation and evolution of this cloud can be made. In the next section the particular translucent cloud which is the focus of this study will be discussed.

---

[6] Galactic coordinates are coordinates based on the galactic plane and are discussed in Appendix A.

Figures for Chapter 1

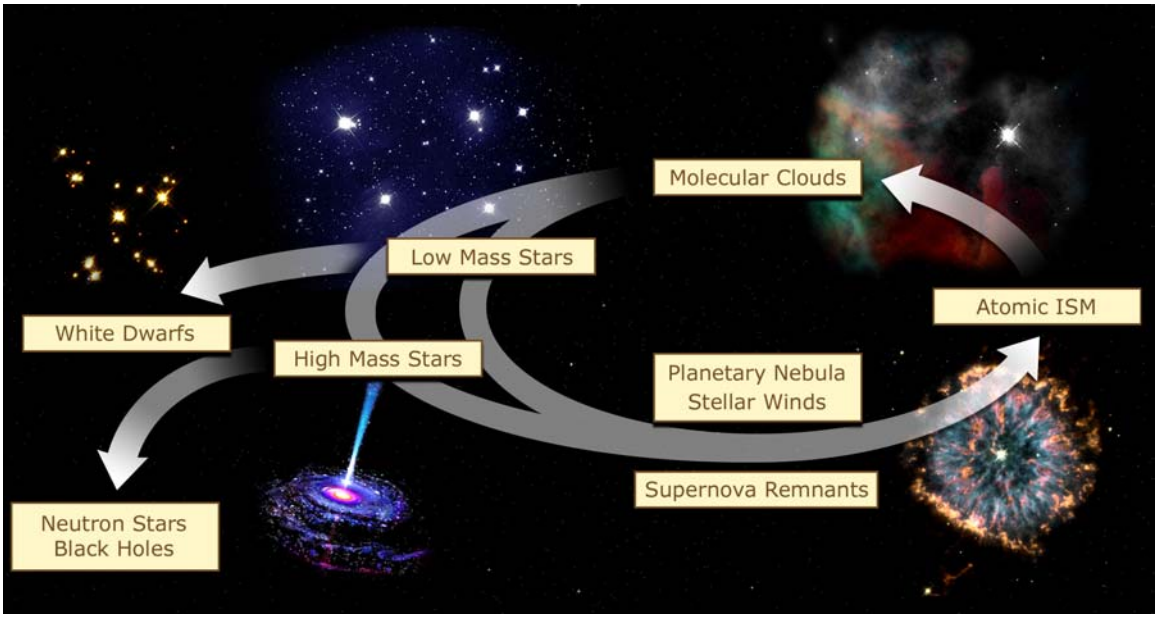

Figure 1.1 – The Star-Gas Cycle.
Picture credits: NASA

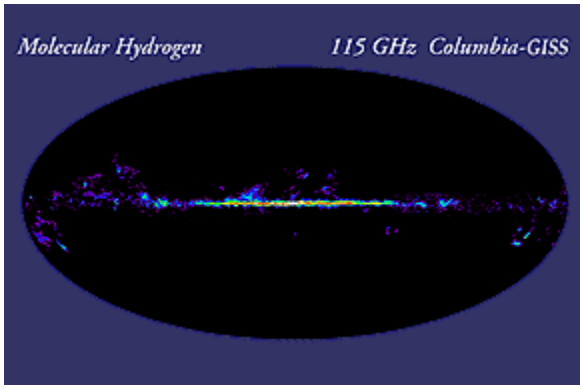

Figure 1.2 – The Milky Way Galaxy H_2 distribution.
Picture credit: NASA, from a composite of
surveys of CO by Dame, Hartmann, & Thaddeus (2001).

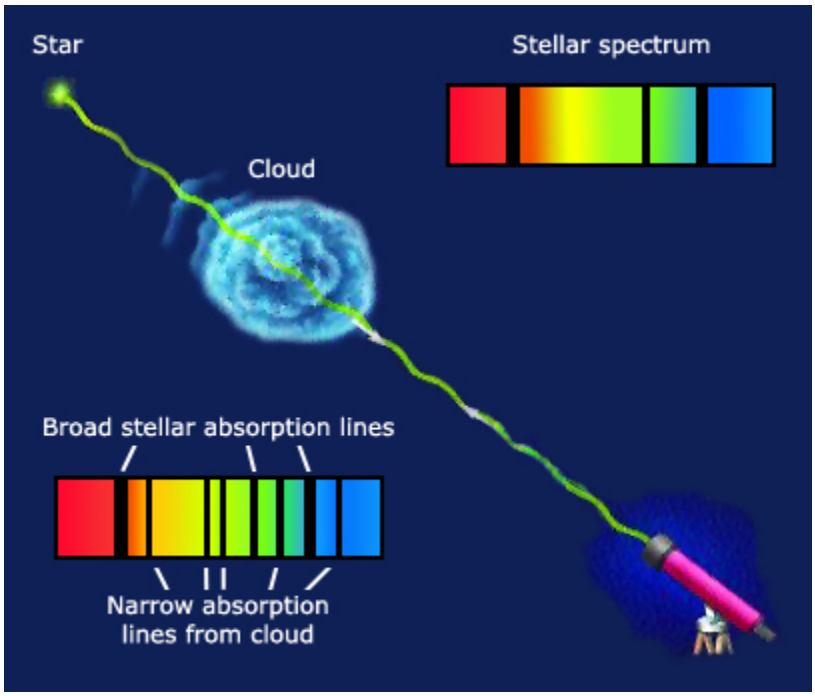

Figure 1.3 Spectral absorption lines of a cloud against a stellar spectrum

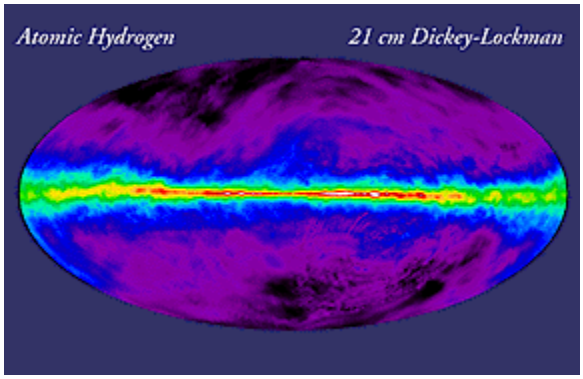

Figure 1.4: The Milky Way galaxy mapped in H I
Picture credit: NASA from the data of Dickey (1990)

Chapter 2 – MBM 40

The translucent high latitude molecular cloud chosen for this study is MBM 40[7], a small (0.7 deg^2), low mass (10-20 solar masses), compact, low-extinction cloud. The cloud is isolated from other molecular features and located at a galactic longitude, l = 37˚.6, and a galactic latitude, b = 44˚.7 (see Appendix A for an explanation of galactic coordinates). MBM 40 is projected on a large feature extending north from the Galactic plane called the North Polar Spur. The North Polar Spur is believed to be an old supernova remnant, and extends from the Galactic midplane up towards the North Galactic Pole. MBM40 is embedded in a complex of dust emission (see Figure 2.1) and its distance estimate is important if we are to determine the physical properties of the cloud.

The distance to high-latitude clouds such as MBM 40 was first established by Magnani, Blitz, and Mundy (1985), who estimated the average distance to the ensemble of high latitude clouds to be ~100 pc. This estimate was based on a statistical analysis of the all cloud velocities in the Magnani, Blitz, and Mundy (1985) survey. Unfortunately, while this estimate is accurate in a general sense for the ensemble of clouds, it says nothing about any individual object. To determine the distance to a given cloud, more direct methods must be used. One way to do this is to take a spectrum of a star behind the cloud. The spectrum will then show broad absorption lines from the stellar

[7] MBM 40 is cloud 40 from the catalog of Magnani, Blitz, & Mundy (1985).

atmosphere and narrow lines from the interstellar cloud (See Figure 1.3). By finding a star in front of the cloud (which obviously would not show the narrow lines), the distance to the cloud can be inferred. In this fashion, an echelle spectroscopy survey of the Na I absorption line by Welty et al. (1989) set an upper limit of 140 pc for the cloud distance. The distance estimate was then improved by Penprase (1993) in a more thorough study of about two dozen foreground and background stars. This yielded a range of 90 - 150 pc for the distance. Thus 120 pc is adopted as the distance to the cloud for the remainder of this thesis.

2.1 History of MBM40 Observations

The cloud was first cataloged (Object 79) and misidentified by Sharpless (1959) as an H II nebulosity. Lynds (1965) studied the immediate vicinity of the cloud and identified two bright nebulae, LBN 105 and 106. However Lynds did not speculate as to what was producing the faint emission on the photographic plates. We now know that this is due to starlight reflecting off the dust contained within the cloud. An H I structure was first identified in the region at v_{LSR}[8] = 4 km s^{-1} by two separate studies, Verschurr (1974) and Colomb, Pöppel, & Heiles (1980). Shortly thereafter, molecular gas was detected by Blitz, Fich, & Stark (1982) during a survey of CO (J = 1-0) emissions from Sharpless objects. However, this detection was only at one position. MBM 40 was finally identified as a distinct molecular cloud and partially mapped by Magnani, Blitz, & Mundy (1985) during their high latitude CO (J = 1-0) survey. The cloud was poorly sampled (10′ sampling with a 2′.3 beam) but its general structure was clearly discernible. A more thorough mapping was done by de Vries (1988), although he called it the

[8] LSR is the Local Standard of Rest.

Hercules cloud. This map, again in the CO (J = 1-0) emission, improved upon the earlier map due to its compete sampling though with a worse resolution (8′.7 beam).

2.2 Basic Properties of MBM 40

Magnani et al. (1996) studied MBM 40 in great detail by analyzing several molecular species and established many of the fundamental physical characteristics of the cloud. By comparing CO, CS, and H_2CO data from the cloud with IRAS 100 μm data, that study established MBM 40 as a translucent, compact cloud with a visual extinction throughout its extent of less than 2 magnitudes. This visual extinction makes MBM 40 an archetypical translucent high latitude molecular cloud, as described in Chapter 1. The mass was established to be in the range of 20 to 40 solar masses, with a principle molecular "ridge" within the cloud having a mass around 20 solar masses. This ridge runs northwest-southeast and has a smaller counterpart to the east making a "wishbone" shape in the principal molecular tracer, CO (see Figure 2.2)[9]. This molecular emission matches the IRAS 100 μm distribution very well – as is expected because the gas and dust are well mixed in the interstellar medium (Spitzer 1978). Within the principal ridge, some dense substructures with volume density $n_{H2} \geq 10^3$ cm^{-3} were detected. The column density of H_2 was established to be $N_{H2} \sim (1\text{-}7) \times 10^{20}$ cm^{-2} (capital N is traditionally reserved for column density in the astronomical literature, and small n represents the volume density).

In addition to this study, van Dishoeck et al. (1991) used multiple CO transitions along with other chemical tracers to probe the properties of four points within the denser sections of the cloud. Their results correspond closely with those of Magnani et al.

[9] In astronomical usage, east is to the left and north is at the top of a given map.

(1996), with $n_{H2} \sim 10^3$ cm^{-3}, and H_2 column densities on the order of $N_{H2} \sim$ (5-8) x 10^{20} cm^{-2}. Gas temperatures were estimated to be ~ 30 K, typical of translucent molecular clouds.

2.3 MBM 40 – Bound or Unbound?

Molecular clouds form stars when clumps within them begin to collapse under their own self-gravity. More specifically, gravitational forces overcome the other forces which are supporting the clump. The supportive forces are generated by magnetic fields and by turbulent gas motions. The origin of the energy source which keeps the turbulent gas motions going is controversial at this time. In Chapter 5, we will argue that in MBM 40 the source of the turbulent gas motions is external to the cloud. In the meantime, we will examine how one can determine whether a molecular cloud as a whole (as opposed to a clump within the cloud) is gravitationally bound (and thus contracting), gravitationally unbound (and thus expanding or breaking up), or gravitationally stable (neither expanding nor contracting but in a long-lived stable equilibrium).

Just as in the case of a clump, an entire molecular cloud can be considered bound if its gravitational potential energy term ($-\frac{3}{5}\frac{GM}{R}$, where G is the gravitational constant, M is the mass, and R is the radius) is greater than its kinetic energy term (proportional to the velocity of gas particles squared). In actuality, a molecular cloud can be thought of as an aggregation of particles so that a virial analysis can be applied. The virial theorem is a description of how the dynamical state of an ensemble of particles changes over time. In the form appropriate for molecular cloud studies, the virial theorem states that 2 times the kinetic energy of the system of particles must be equal to the gravitational potential

energy. In this case, the system is said to be in virial equilibrium and it is neither expanding nor contracting.

The question for MBM 40 is how does its overall kinetic energy compare to its gravitational potential energy? Magnani et al. (1996) examined this question and determined that the kinetic energy term was somewhat larger than the gravitational potential energy term. The two were close enough that MBM 40 might be gravitationally bound; however, a more complete analysis by Shore et al. (2003) indicates that MBM 40 is not gravitationally bound. The implication of this fact is that the cloud is not a long-lived structure and is breaking up on the timescale of a million years. This will be discussed further in Chapter 5.

2.4 Star Formation in MBM 40

The possibility of star formation in MBM 40 was eliminated after exhaustive study by Magnani et al. (1996). Several clumps of gas found within the cloud resemble the standard low mass cores described by Myers (1985), but the volume densities indicated by the CO and H_2CO observations were at least one order of magnitude too small. Further multiwavelength examinations of the cloud (Hearty 1998) established that there was no recent or ongoing star formation within MBM 40, with the lack of x-ray sources being the key consideration for deciding that MBM 40 is not forming stars (x-ray point sources in molecular clouds are almost always produced by young, newly formed stars). The study by Hearty (1998) concluded that the gravitational binding of the clumps was not sufficient to initiate star formation.

Figures for Chapter 2

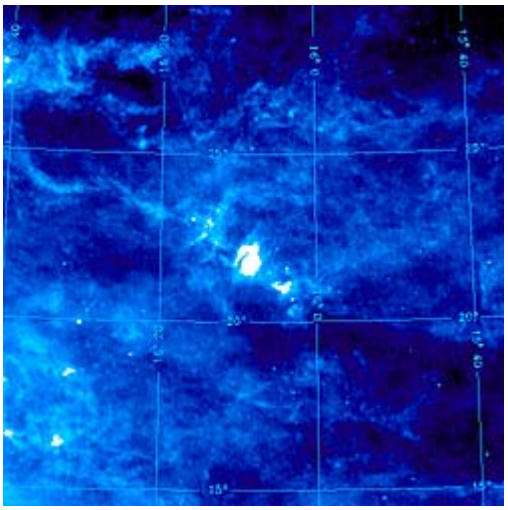

Figure 2.1 IRAS 100 μm survey of the MBM 40 region.
IRAS is the Infrared Astronomy Satellite (Low, 1984).
MBM 40 is the bright white region in the center of the map. The map extends 15˚ x 15˚.

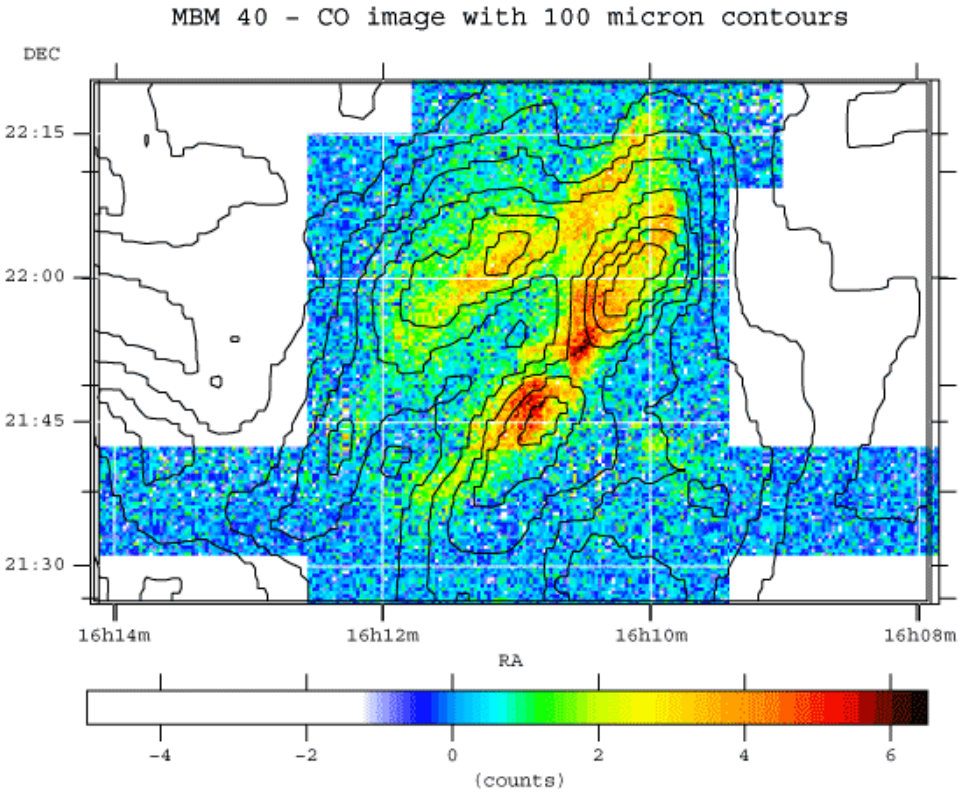

Figure 2.2 The CO morphology of MBM 40 in color with IRAS contour overlay.

Chapter 3 – The Atomic Hydrogen Observations

The high latitude molecular gas cloud MBM 40 was described in Chapter 2 and is an ideal target for an atomic hydrogen –molecular hydrogen comparison because of its location above the confusion of the Galactic plane. By comparing the morphology of the atomic map with a previously made molecular map of the cloud, it is hoped that a conclusive picture of how the cloud formed can be determined.

The H I map is made by detecting the emission of radiation by the neutral hydrogen atoms when they spontaneously de-excite from a state of higher energy to one of lower energy. This emission is detected at 1420 MHz, which is equivalent to a wavelength of 21 cm, and thus falls into the radio part of the electromagnetic spectrum. The data were obtained at Arecibo Observatory, which is part of the National Astronomy and Ionosphere Center, a national research center operated by Cornell University under a cooperative agreement with the National Science Foundation. Arecibo Observatory is the site of the world's largest single dish radio telescope, with a fixed 305m diameter spherical reflector, and moveable feeds overhead. The H I data were taken during the summer of 2001 and reduced into maps during the summer of 2002. The H I maps will be presented in Chapter 4. In this chapter, I will discuss the mechanism by which H I produces 21 cm radiation and how this is detected using the Arecibo radio telescope.

3.1 The Atomic Hydrogen Emission Line

Neutral hydrogen gas is one of the primary components of the interstellar medium, with an approximate density in the Galaxy of 1 atom/cm^3. An input of energy into hydrogen gas can cause energy level transitions in the optical or UV portions of the spectrum if the energy is sufficient to populate the relevant states. The dense interstellar medium is too cool to populate these states, but the gas does have a strong spontaneous emission feature at the 21 cm wavelength. This radio emission is produced by the spins, or angular momenta, associated with the proton and orbiting electron of the hydrogen atom. The proton and electron are both spinning distributions of opposite electric charge, and the spinning charge produces minute magnetic fields which then interact with each other. The hydrogen atom can either be arranged in a parallel formation, with both spins in the same direction, or an antiparallel formation, where the spins are in opposite directions. The state where the spins are aligned is at a slightly greater energy level than the antiparallel formation (see Figure 3.1).

Approximately once every 500 years, hydrogen atoms in an atomic cloud collide, which results in the atom being excited into its higher energy state with the spins of the proton and electron aligned. An undisturbed hydrogen atom will stay in this state for as long as 30 million years before it spontaneously decays into its lower energy state via a spin-flip, where the electron will change its spin orientation. The photon released from this flip will have an energy exactly equal to the difference in energy between the parallel and anti-parallel state of the electron. This photon is emitted as 21 cm radio (1420 MHz) emission. The fact that this emission line is readily detectable by radio techniques is a testament to the high H I column density in all directions of the Galaxy. The 21 cm line

was the first radio spectral line to be detected from the Galaxy (Ewen & Purcell 1951; Muller & Oort (1951). Even today, it remains the most readily detectable spectral line in the interstellar medium.

3.2 The Arecibo Observatory – An Overview

In order to detect the 21cm line a radio telescope which can be tuned to the frequency 1420 MHz is needed. The neutral hydrogen emission data was collected using the Upgraded Arecibo 305 meter radio telescope near Arecibo, Puerto Rico (see Figure 3.2). Arecibo is the world's most sensitive radio telescope because it has the largest reflecting surface. The primary reflecting surface is the aluminum 305 m dish suspended above the ground in a natural depression in the limestone karst formations of Puerto Rico. While it was originally built for incoherent scattering radar experiments, there have been two upgrades which have greatly increased the versatility of the observatory. From 1972-1974 the spherical primary reflecting surface was changed from a thin wire mesh to aluminum paneling, which allowed the telescope to observe at higher frequencies (up to 2-3 GHz). The second upgrade occurred in 1997, which replaced the line feed receivers (explained below) with the Gregorian dome. The Gregorian dome corrects for the spherical aberration of the reflecting surface and allows for observations of spectral lines up to 10-12 GHz. In addition, a ground screen was built to reduce spillover noise, and dynamical tie-downs were installed to stabilize the position of the aerial platform. These upgrades, in addition to the sensitivity of the Arecibo telescope, make it ideal for this study of the 1420 MHz emission of neutral hydrogen in MBM 40.

The primary reflecting surface at Arecibo is a 70˚ spherical cap of aluminum panels which collects the radio signals from the target. This dish cannot be moved, so tracking of targets is done by changing the angle of the receivers suspended above the dish. There are two types of receiver configurations at the Observatory: line feeds and horn antennae, the latter of which are housed within the Gregorian dome. Because the surface of the dish is spherical, it can cover a larger area in the sky than a more traditional parabolic reflector. However, this means that the signal reflected by the dish comes to focus above the dish in a line, rather than at a single point. Thus, line feeds, which are large waveguides, can be placed in these lines of focus, and collect the signal at all of those points along the line. Alternately, the line of signal can be reflected additional times in order to correct for this spherical aberration. The Gregorian dome contains two shaped mirrors which collect and reflect the signal to a single point, as shown in Figure 3.3. With this correction, the signal can then be measured by a variety of collectors, each sensitive to specific wavelengths, which are mounted on a turntable within the Gregorian Dome.

Of course, whether one is using the Gregorian or the line feed systems, the metal "arm" the two types of feeds move on is limited to pointing at objects which pass within 20˚ of the zenith. This explains why the Arecibo telescope is situated in Puerto Rico. A moment's thought will reveal that the greatest area of the sky that can been seen if one is limited to a certain number of degrees from the zenith is at the equator. As the Earth turns on its axis, more sky is covered at the equator than at the poles. Thus, the telescope had to be placed on the United States possession which was nearest to the equator and had reasonable infrastructure to support a project of this magnitude. The island of Puerto

Rico, a U. S. territory since the Spanish-American War of 1898, is at a latitude of 18˚ North and thus was chosen to house the world's largest radio telescope. If the feeds can reach within 20˚ of the zenith, the location of Puerto Rico at a latitude of 18˚ N ensures that all celestial objects with declinations (see Appendix A) between (18˚ – 20˚) = -2˚ and (18˚ + 20˚) = 38˚, can be observed from Arecibo. The cloud MBM 40 is ideally suited for this since its declination is 22˚.

The Arecibo Observatory is under the National Astronomy and Ionosphere Center (NAIC), and, as the name implies, a wide variety of science occurs there in addition to H I observations. Approximately 75% of the research time at the observatory is dedicated to radio astronomy, which includes galactic and extragalactic astronomy, pulsar observations, and Very Long Baseline Interferometry. Another 10% of the time is for planetary studies such as comets, cateroids, and planetary surfaces, and the final 15% is for space and atmospheric science. The observatory can operate from 50 megahertz (6 m wavelength) up to 10,000 megahertz (10 GHz, or 3 cm wavelength) and may even go to 15 GHz in the future. In addition to simply detecting radio signals, it can transmit its own radio signals towards objects of study, and then detect the returning radar scatter. Observing time at the Observatory is obtained by anonymous peer-review of proposals. Prof. Loris Magnani of the University of Georgia submitted a proposal in the summer of 2000 to make H I observations of the vicinity of the MBM 40 cloud. The time was granted and observations were scheduled for 2001.

3.3 The Arecibo Observatory – Data Collection and Reduction

The H I data were taken over a four week period in May and June 2001 at the Arecibo Observatory. The receiver used was the L-narrow dual polarization receiver, which at 1420 MHz has a beamwidth of 3.1′ x 3.5′ with a sensitivity of 8-10 K/Jy. The beamwidth signifies the area of the sky that is sampled by each pointing of the telescope. Details smaller than 3.5′ can not be discerned by the Arecibo radiotelescope at the frequency of 1420 MHz. A complete list of characteristics of the 1420 MHz system at Arecibo is detailed in an Arecibo internal memo (Heiles et al. 2000). The data were taken by dividing the cloud and its vicinity into a grid with 32 separate pieces, or subgrids, with each subgrid covering a 0.5˚ x 0.5˚ region of the sky. The subgrids covered the cloud with 8 subgrids along Right Ascension and 4 subgrids along declination. Thus a 4˚ x 2˚ region of the sky ($15^h\ 58^m < \alpha < 16^h\ 14^m$ and $21.0^\circ < \delta < 23.0^\circ$ in 1950.0 coordinates) centered on MBM 40 was covered. Within the grid, the data were taken in a raster pattern along Right Ascension, with each row being 30′ in length. Fifteen spectra comprised each row, with 17 rows per grid, giving a total of 255 spectra per grid or 8160 spectra for the entire map. The sampling was effectively ½ the beamsize and this was done to ensure complete coverage of a given region. The bandpass shape was distinct and stable from grid to grid. The autocorrelator[10] was divided into four sections, two of each polarization for redundancy. Each section had 2048 channels and 3.125 MHz bandwidth. What this means is that each spectrum covered the equivalent of 660 km s^{-1} in velocity, centered at 0 km s^{-1} with respect to the LSR. Each spectrum was composed of 2048 channels, giving

[10] An autocorrelator is a device which takes the radio power as a function of frequency and produces (via Fourier transform) power as a function of frequency. The latter is, after calibration, the spectrum.

a velocity resolution of 0.32 km s^{-1} (660 km s^{-1} / 2048 channels). Final maps were produced by adding the two polarizations.

The data was reduced at Arecibo in August of 2002 using IDL and Arecibo software written primarily by Phil Perillat and Snezana Stanimirovic. This software calibrated, gain-corrected, and converted the spectra into a three dimensional datacube (Right Ascension, declination, and v_{LSR}). The data cube is described in detail in Chapter 4. The data reduction procedure is roughly as follows. Each day, the data were collected in a file called the correlator file. The correlator file contains all the spectra from the 2 or 3 subgrids which were observed on any given day. All the spectra in the correlator file are calibrated in units of antenna temperature, a traditional measure of the radio power detected by the radio telescope. The radio power from the source sits on top of the radio power produced by the electronics. This latter power sometimes has a structure as a function of frequency which can be removed by fitting a high order polynomial to the structure. This is called baselining the data and all the spectra were baselined in this function. A typical spectrum is shown in Figure 3.4. The reduced output file is gain corrected, a procedure which accounts for the differing sensitivities of different parts of the reflecting surface, and then the files are combined into a larger map. Finally, the larger map is regridded to smooth out any sampling irregularities, and the spectra are stored in a datacube. The next chapter will describe datacubes and present the data itself.

Figures for Chapter 3

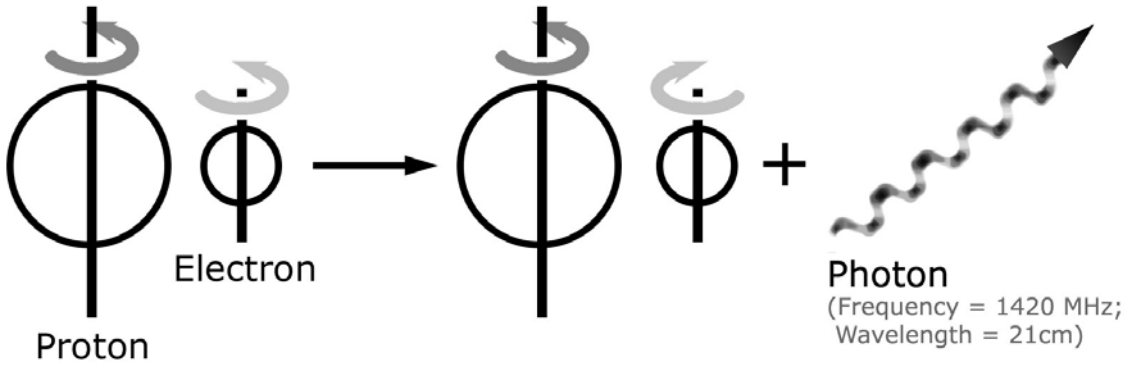

Figure 3.1 The spin-flip emission of neutral Hydrogen at 21 cm.

Figure 3.2 The Arecibo Radio Telescope

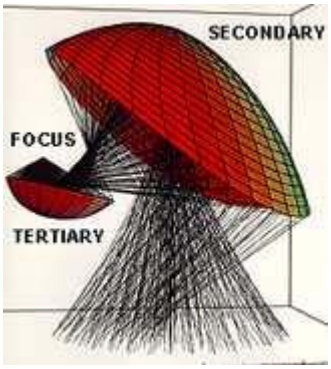

Figure 3.3 The secondary and tertiary reflecting surfaces contained within the Gregorian dome.

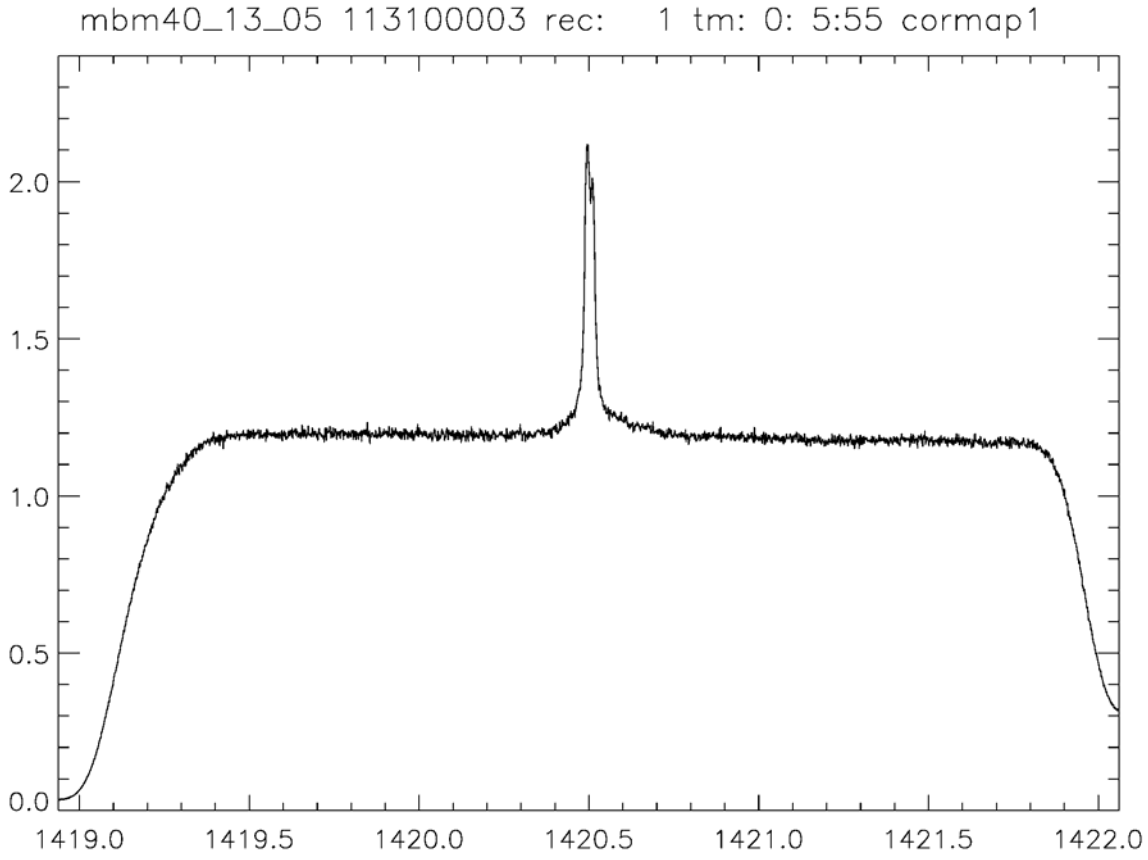

Figure 3.4 A typical raw H I spectrum before any data reduction. The scale is correlator units versus frequency.

Chapter 4 – The Atomic Hydrogen Data for MBM 40

4.1 The Data Explained – From Spectra to Datacube

The H I data taken at the Arecibo Observatory during the summer of 2001 was reduced (as described in Chapter 3) into a three-dimensional datacube with dimensions Right Ascension, Declination, and velocity with respect to the LSR. The datacube structure takes advantage of the fact that each spectra taken contains information on the velocity distribution of the material. As described in the previous chapter, the H I spectra are plots of the radio power as a function of frequency. The frequency axis is split up into bins, which are called channels. Each channel of our data was 1.5 kHz wide which corresponds to 0.32 km s^{-1} at the frequency of H I. At high galactic latitudes, typical H I spectral lines are 10 - 20 km s^{-1} wide, so that our signal will appear over several dozen channels (recall that the entire spectrum is 2048 channels wide, equivalent to 3.125 MHz or 660 km s^{-1}).

When one combines the data from all the spectra to create a map of the region, one can plot the area under the H I line for each sampled position. This would produce a map of the total intensity of H I, which would be proportional to the column density of H I (see section 4.3). If instead of the integrated line profile, one plots the power for a given channel over the entire sampled region, then one has a map of the H I at a given velocity. Thus, not only can the quantity of H I within the cloud be determined, but the kinematics

of the gas within the cloud can also be described. This section will fully explain the structure and advantages of the datacube, followed by the H I data of MBM 40.

As described above, traditionally, the area under the spectral profile (refer back to Figure 3.4) can be calculated and assigned as the value of intensity at that particular position of the sky, and this area is proportional to the H I column density of the cloud. This produces a two-dimensional map of the intensity of the specific spectral line. To visualize this better, one can imagine that each pixel of the map (corresponding to each pointing of the telescope) contains the value of the intensity of one spectrum, which has been assigned some color to signify its value with respect to neighboring pixels. This type of position versus position map is shown in Figure 2.2.

As pointed out above, the spectra contain more than the total intensity. By plotting the third dimension as velocity, or, alternatively, by making each position by position map at a single velocity and then stacking those position maps consecutively in order of velocity, a position, position, velocity datacube is formed. By including the velocity, information about the radial motions and hence the kinematics of the gas within the cloud can be determined.

The MBM 40 datacube can be described as follows. A 4° x 2° region extending from $15^h58^m.0$ to $16^h14^m.0$ in right ascension and 21°.0 to 23°.0 in declination (1950.0 coordinates) was mapped. When all the data were combined, a map with 120 x 60 pixels of data was created (the 8160 spectra had some overlap in declination so that only 7200 positions were actually sampled). Each pixel is represented by a spectrum and, since each spectrum has 2048 channels, a datacube with dimensions 120 x 60 x 2048 was created. Thus one can choose any one of the 2048 channels to view, and see the intensity

value for that particular channel for all 120 x 60 positions (or pixels). Most of the channels will simply be noise, since the H I line is contained only in a narrow range of channels. The area with the line is a region of about 40 consecutive channels, which corresponds to ~12 km s^{-1} wide. These relevant channels are designated as channels 1005 through 1045, which cover the velocity range of -6 km s^{-1} to +6 km s^{-1}. Plotting the intensity at each channel shows the pattern of the global velocity changes within the cloud, in turn, reveal the kinematics of the cloud.

4.2 The H I Maps

Reproduced in Figure 4.1 are the 40 slices of the data cube for each of the channels containing the H I signal. Each individual map covers the same region of the sky but at different velocities. Table I gives the relationship between the listed channel number and the equivalent velocity with respect to the LSR.

The antenna temperature is given by the color bar at the bottom of each page and is in units of K. The conversion from units of antenna temperature to H I column density is described in section 4.3.

The molecular gas in MBM 40 extends from 2 – 4 km s^{-1} (Magnani et al. 1996) and the atomic hydrogen associated with the cloud is clearly seen as the "blob" feature in channels 1006 - 1016. The other morphological features of the H I environment of MBM 40 are discussed in Chapter 5.

Figure 4.2 shows the H I map of all the velocity channels summed together (i.e., the total intensity map, or the map of the total area under each spectrum).

Figure 4.3 shows the H I map over channels 1013 – 1016 (i.e., those channels with velocity corresponding to the velocity of the molecular emission).

4.3 Deriving the Column Density from the H I Maps

In order to get the column density of H I from the intensity maps, two steps must be taken. First, the intensity data must be corrected for the fact that Arecibo is not a perfect radio telescope. Thus, the quantity measured, the antenna temperature, depends upon the properties of the antenna. For Arecibo, at the time the data were taken, the antenna temperature has to be scaled up by a factor of two to yield the true radio power. The corrected antenna temperature is called the brightness temperature. To convert from brightness temperature to H I column density (N(H I)), the following formula is used:

$$N(HI) = 1.823 \times 10^{18} \sum_{i=1}^{n} T_{b_i} \Delta v \ \ cm^{-2}$$

T_{bi} is the brightness temperature in channel i and Δv is the width of the channel in units of km s^{-1}. For our data $\Delta v = 0.32$ km s^{-1}. The index runs from 1 to n where n is the number of channels over which the calculation is desired. In this way, the H I column density can be calculated from the figures presented for either the total intensity (Figure 4.2) or for any combination of consecutive channels (Figure 4.1).

Table I: Channel Number and Corresponding LSR Velocity

Channel	v_{LSR} (km/s)		Channel (cont.)	v_{LSR} (cont.)
1005	6.12		1026	-0.64
1006	5.80		1027	-0.97
1007	5.47		1028	-1.29
1008	5.15		1029	-1.61
1009	4.83		1030	-1.93
1010	4.51		1031	-2.25
1011	4.19		1032	-2.58
1012	3.86		1033	-2.90
1013	3.54		1034	-3.22
1014	3.22		1035	-3.54
1015	2.90		1036	-3.86
1016	2.58		1037	-4.19
1017	2.25		1038	-4.51
1018	1.93		1039	-4.83
1019	1.61		1040	-5.15
1020	1.29		1041	-5.47
1021	0.97		1042	-5.80
1022	0.64		1043	-6.12
1023	0.32		1044	-6.44
1024	0.00		1045	-6.76
1025	-0.32			

Figures for Chapter 4

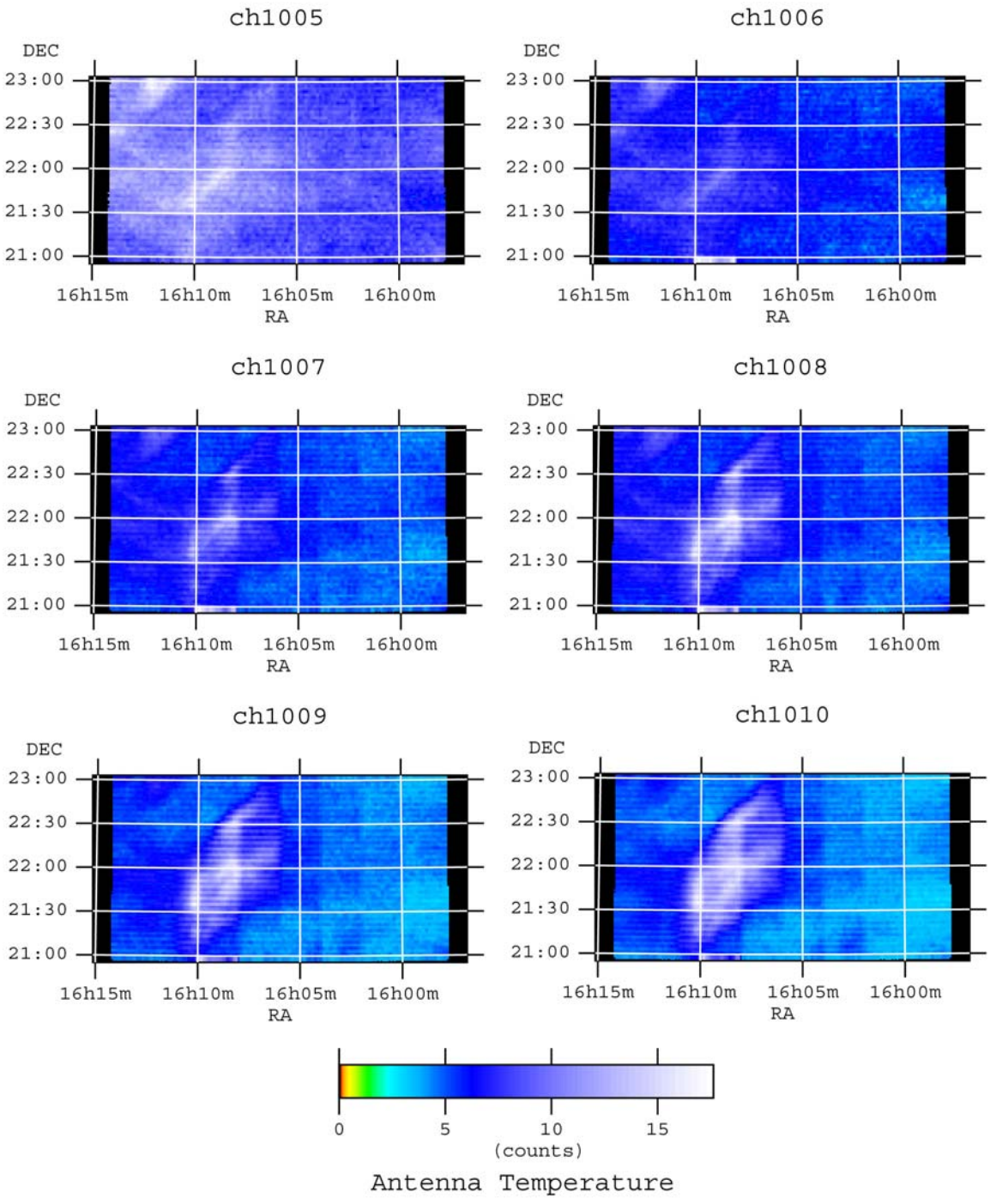

Figure 4.1a MBM 40 H I velocity maps – Channels 1005 - 1010

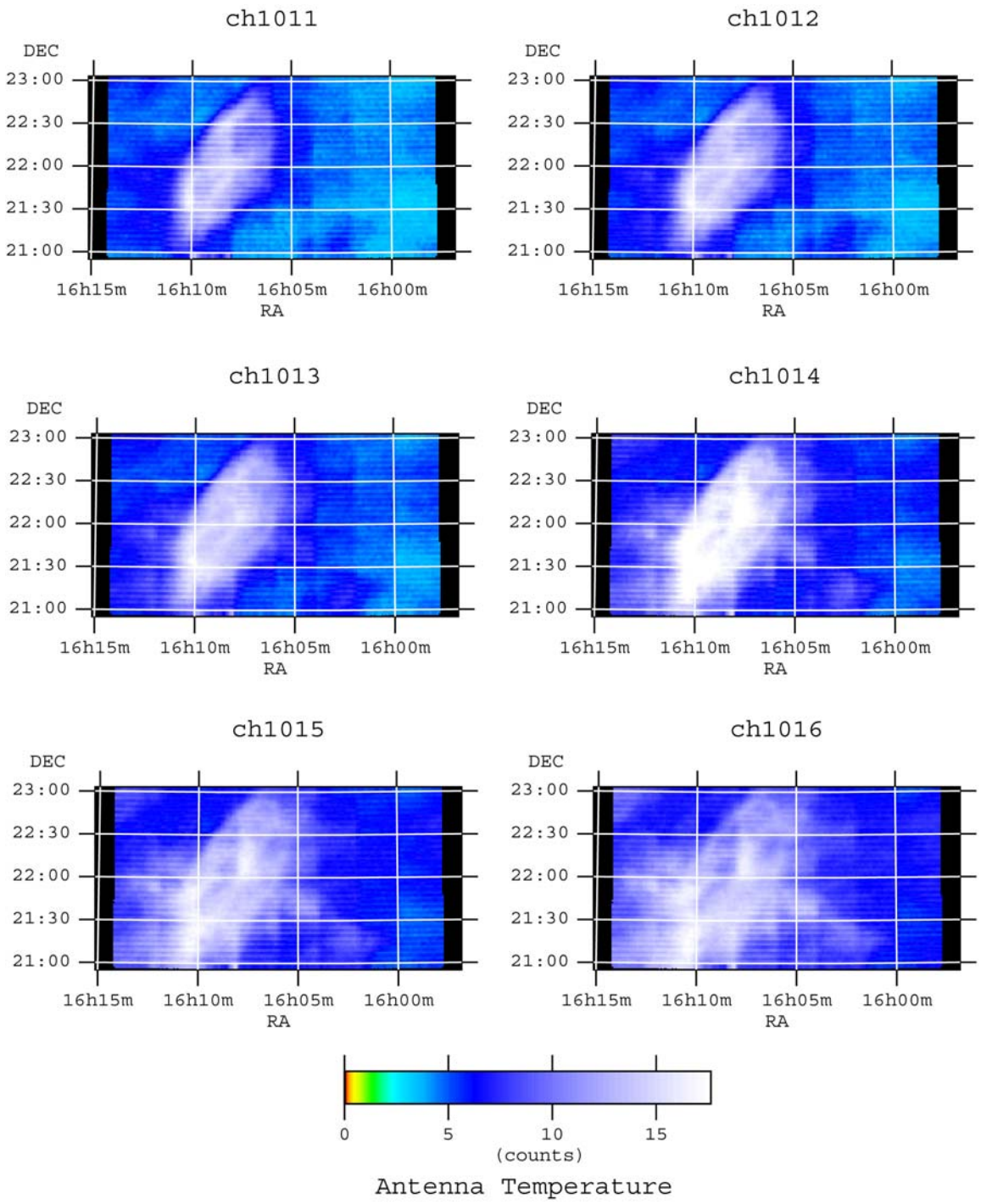

Figure 4.1b MBM 40 H I velocity maps – Channels 1011 - 1016

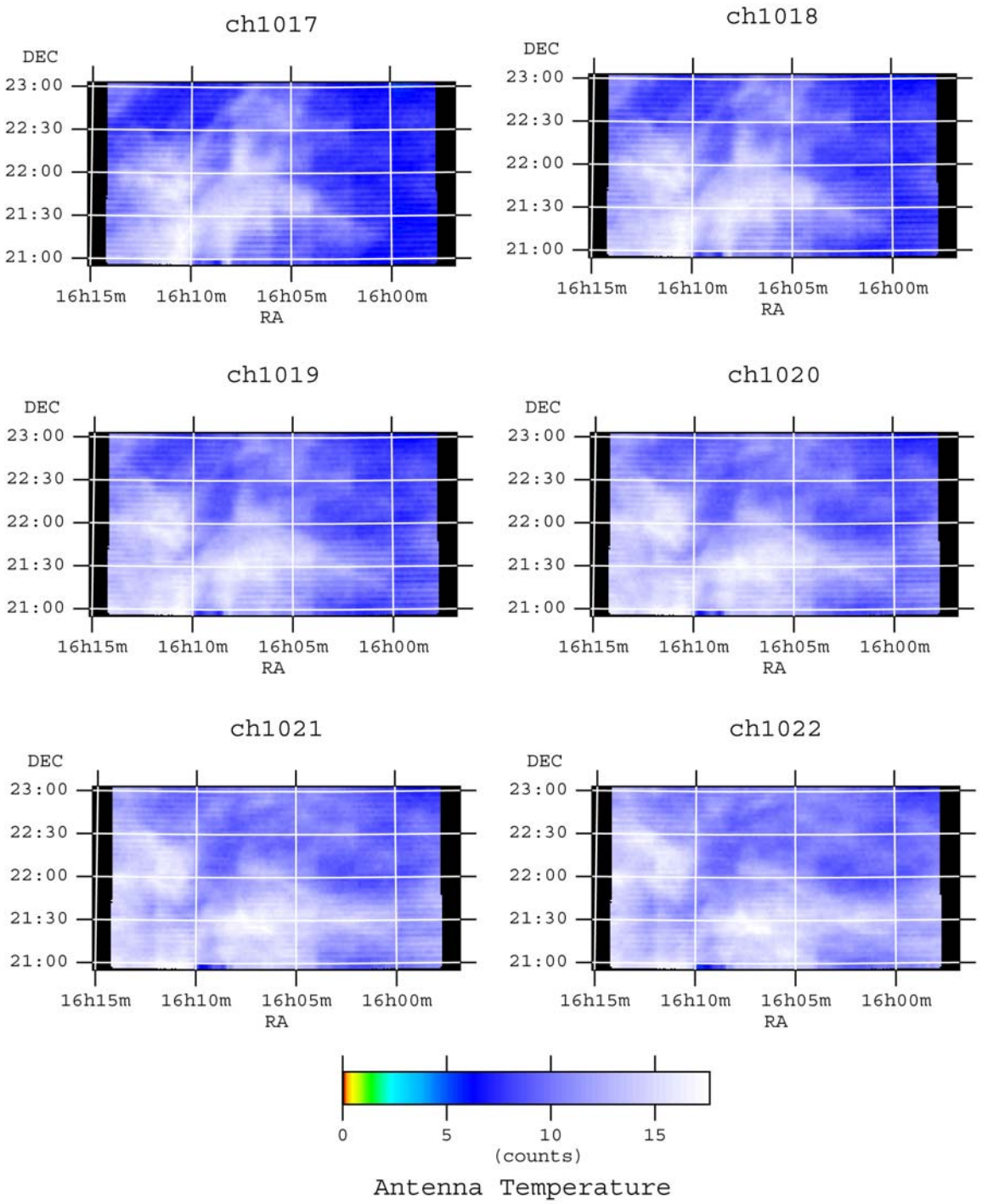

Figure 4.1c MBM 40 H I velocity maps – Channels 1017 - 1022

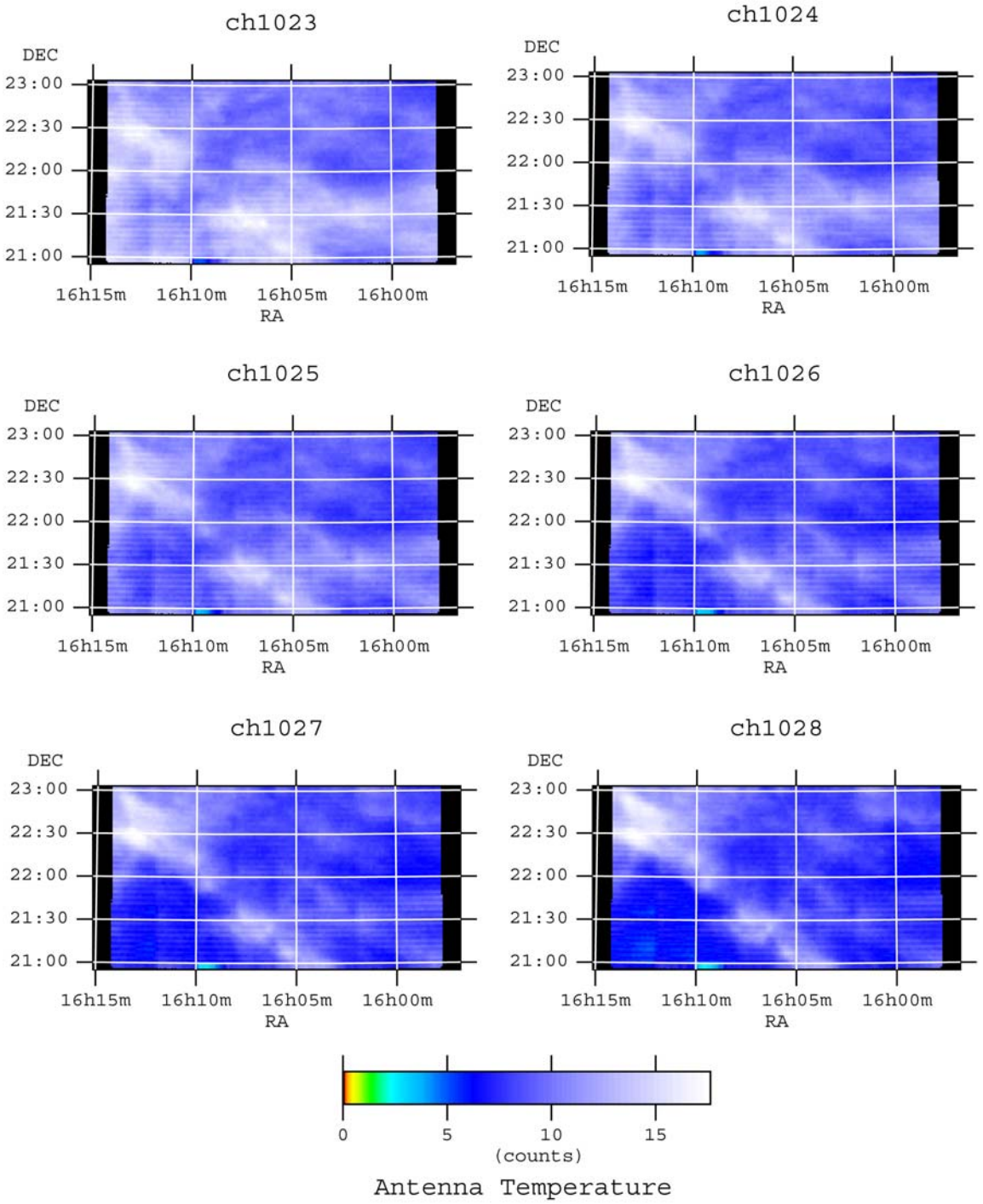

Figure 4.1d MBM 40 H I velocity maps – Channels 1023 – 1028

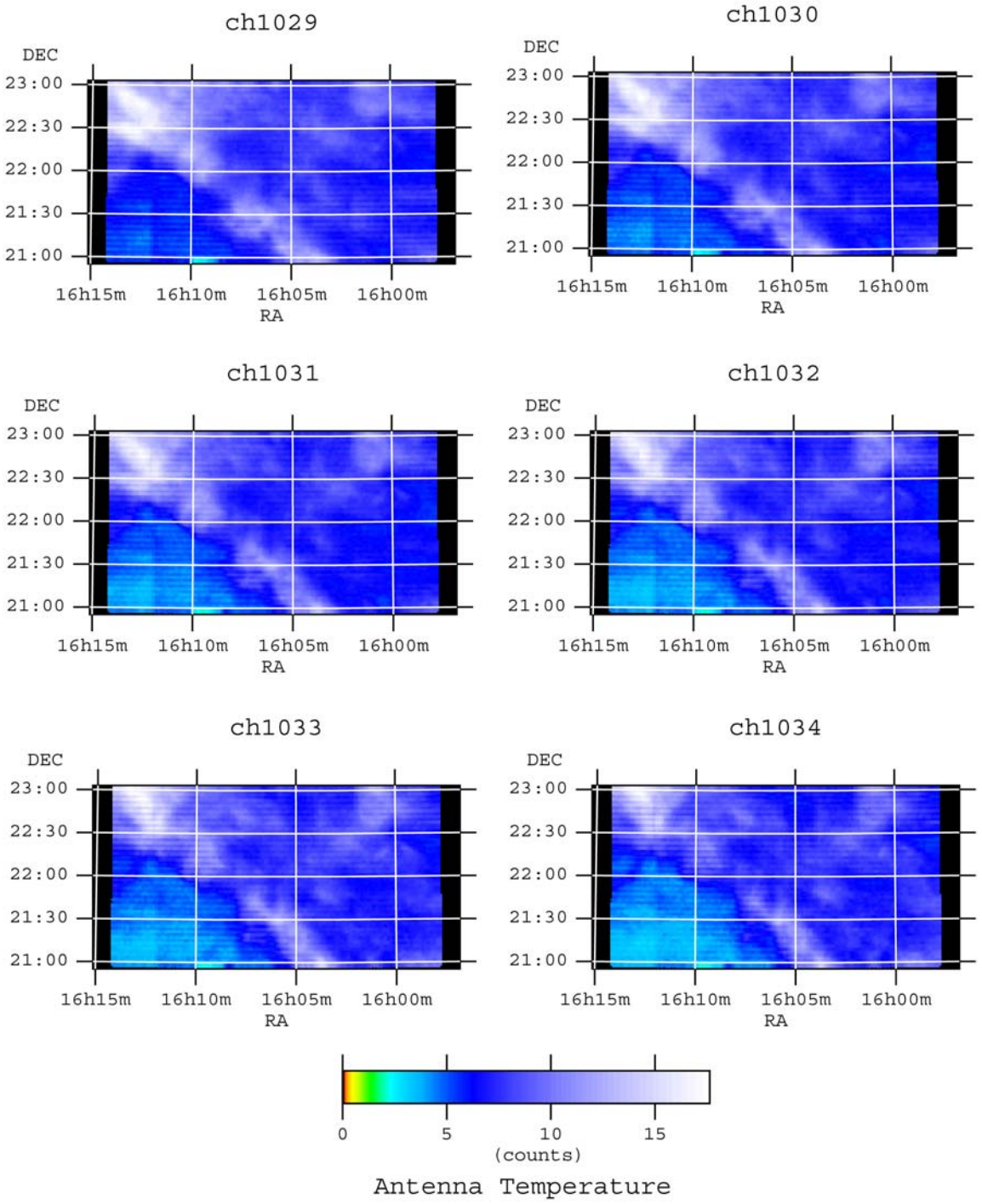

Figure 4.1e MBM 40 H I velocity maps – Channels 1029 – 1034

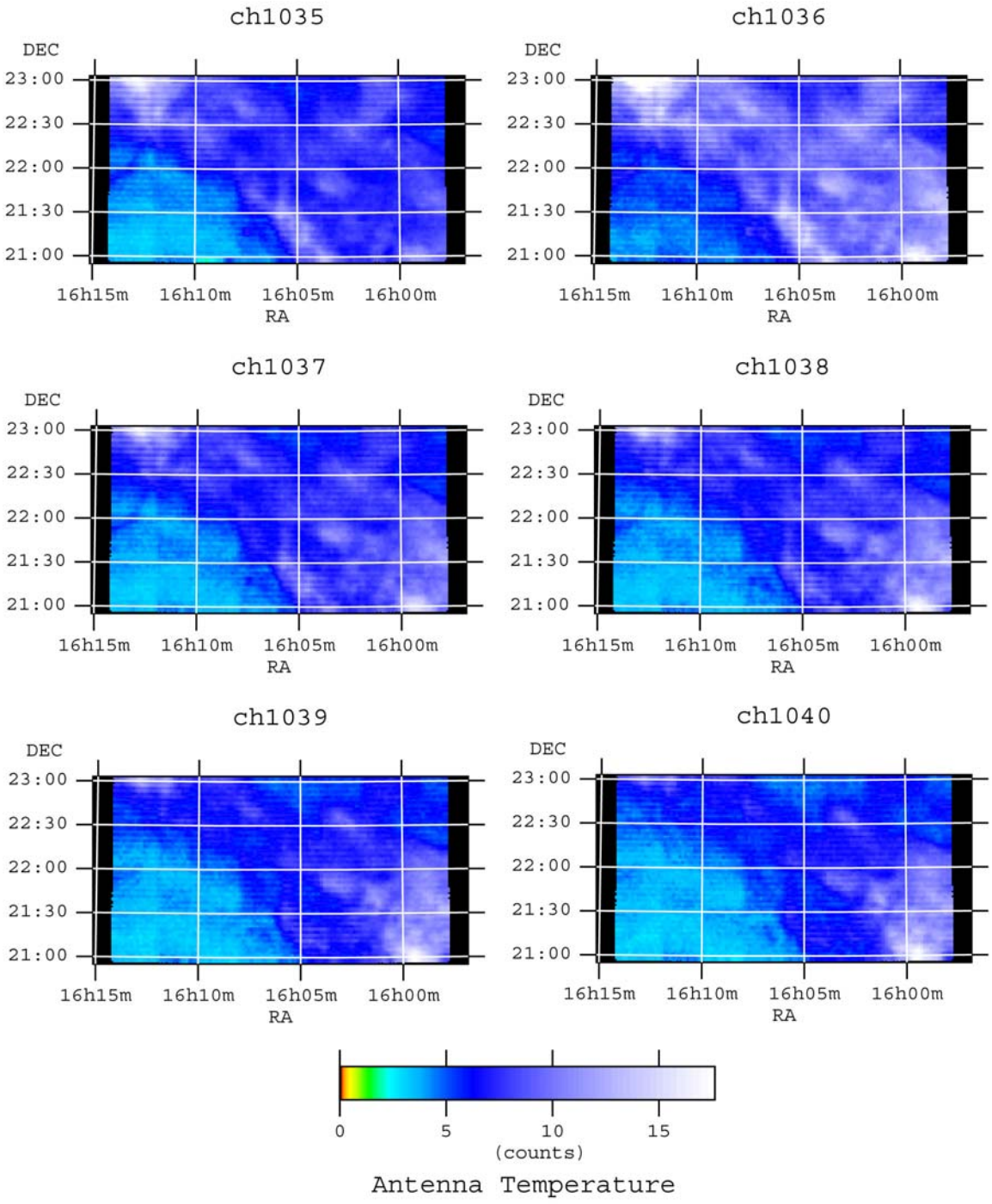

Figure 4.1f MBM 40 H I velocity maps – Channels 1035 – 1040

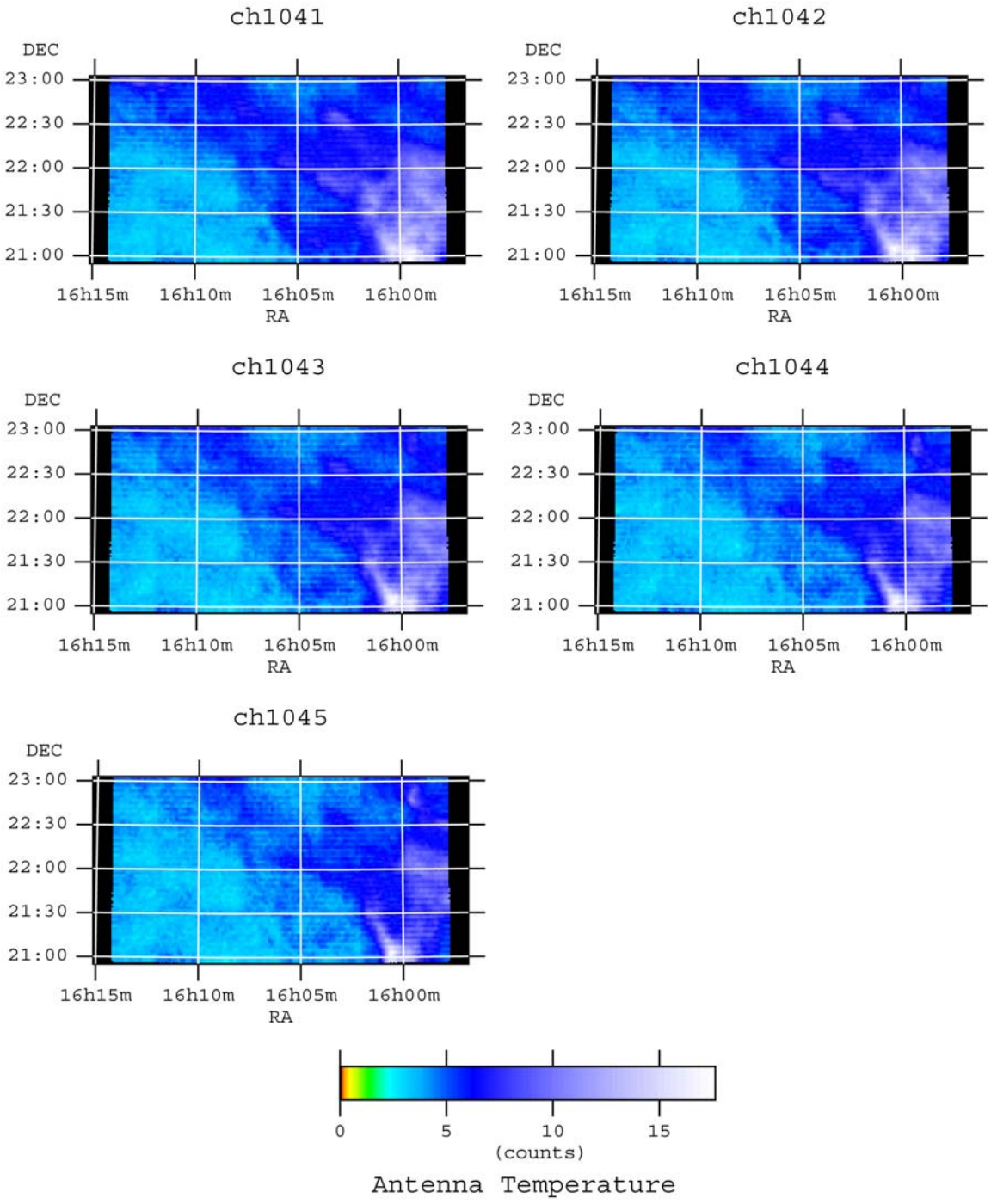

Figure 4.1g MBM 40 H I velocity maps – Channels 1041 - 1045

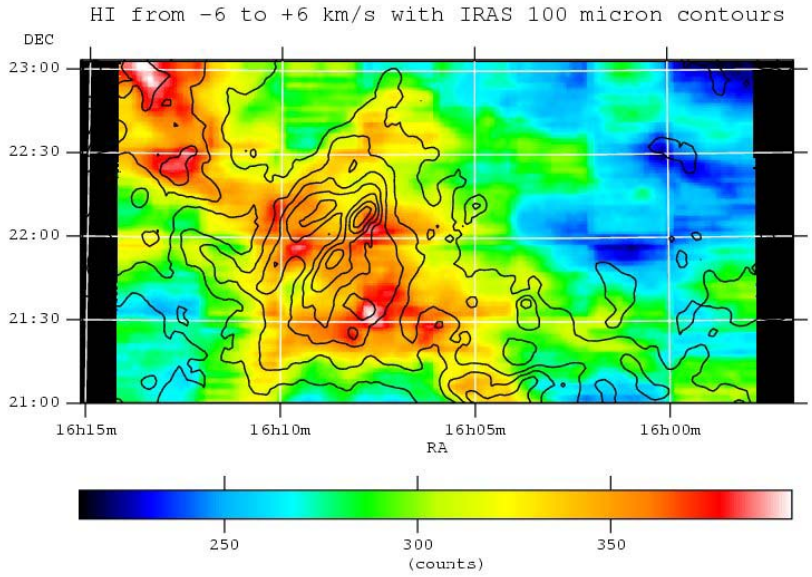

Figure 4.2 H I data of MBM 40 from –6 to +6 km/s in color with IRAS 100 micron contours

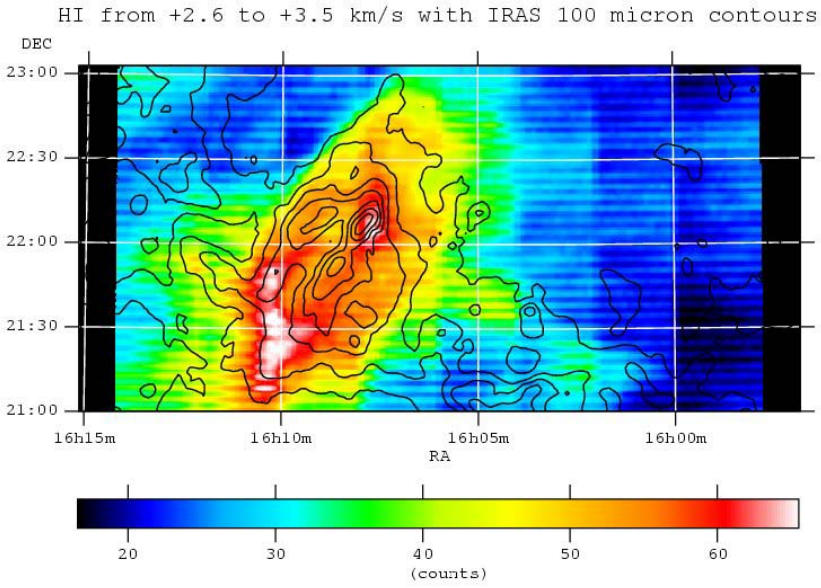

Figure 4.3 H I data of MBM 40 from +2.6 to +3.5 km/s in color with IRAS 100 micron contours superimposed.

Chapter 5 – Interpretation and Conclusions

The intention of this study is to understand as to how a translucent, high-latitude molecular gas cloud, like MBM 40, can form from the atomic interstellar medium. Thus, the H I data presented in Chapter 4 is used in conjunction with molecular data from previous observations to obtain a coherent picture of the gas in this region. Since MBM 40 is one of the simplest high latitude molecular clouds, we have a chance of understanding the manner it may have formed, and perhaps extending these ideas to more complicated clouds. First, the H I data will be examined to explain the trends and structures seen within the cloud, and then it will be argued that shear flows are the driving force behind MBM 40. The discussion in this chapter is presented in greater and more technical detail in the paper by Shore, Magnani, LaRosa, and McCarthy (2003).

5.1 Behavior and Appearance of MBM 40

The H I data, which was presented in Chapter 4, shows the structure of MBM 40 and how it changes at different velocities. The atomic environment associated with MBM 40 progresses through a series of systematic, smooth structural changes. Between the velocities of +6 km s^{-1} and +2 km s^{-1} (Channels 1005 through ~1017 in Figure 4.1) there is a "bubble", or shell, of H I which can be clearly associated with the molecular gas due to their similar morphologies. This atomic shell or envelope surrounds the molecular region (as seen in the contours on the H I maps), and starts to break up and lose it

structure around +2 km s^{-1}. Following the shell at lower velocities (+1 km s^{-1} to -3 km s^{-1}), a bar structure appears gradually, extending from the northeast to the southwest in the left-hand side of the map, along with background and foreground H I which is probably not associated with the molecular cloud. At this point, it is difficult to determine which H I is directly associated with the cloud, and which is part of the flow of H I through the region. For velocities in the range -3 km s^{-1} and -6 km s^{-1}, the H I is seen principally in the right-hand side of the map, and given their location and velocities, these structures are almost surely unrelated to MBM 40.

5.2 The Origin of MBM 40

A molecular cloud needs some form of energy input in order to keep the gas "stirred up" and thus prevent gravitational collapse of some or all portions of the cloud. This "stirring" or energy injection can come from star formation within the cloud, or externally via turbulent gas flows in the H I surrounding the molecular cloud. As was discussed briefly at the end of Chapter 1, two basic theories for forming low-mass molecular clouds exist: formation by shocks, and formation by shear flows.

Shocks form molecular clouds from H I by compression, literally sweeping up atomic gas and dust like a snowplow. The now dense, swept up atomic gas and dust efficiently keeps out ultraviolet radiation (which breaks up molecules) and molecular formation begins in this region. Shear flows work in a different way. A portion of the interstellar gas streams by another and, at the interface between the two flows, turbulence creates instabilities which cause density gradients within one of the flows (usually the more quiescent one). At this point, the denser portions of the flow produce molecular

hydrogen and other molecules because these regions are shielded from the interstellar radiation field (because they are denser than their surroundings). Both shocks and shear flows can inject energy into the dense medium they create and can keep it from collapsing. Since MBM 40 has been shown to have no star formation, external shocks or shear flows must be responsible for its continued support against gravity.

From the literature, it can be seen that in clouds which are parts of large H I shells or fragments of shells, or swept up H I features from the Galactic plane, shocks play a dominate role in their formation and morphology (Gir, Blitz, & Magnani 1994; Bhatt 2000). MBM 40 is not obviously part of such a structure (refer back to Figure 2.1 for the IRAS 100 μm map of the region surrounding MBM 40). In addition, shocks can cause regions of velocity discontinuity within an H I structure, so there should be some evidence of this kind of structure within a cloud condensed by shocks. There is no such edge in MBM 40. Finally, shocks should produce spectral line profiles of different widths as they compress portions of the gas. MBM 40 does not show any evidence of molecular line profiles of different width (Shore et al. 2003). Thus, there is no evidence for shock processes at work within MBM 40.

The H I data is consistent with the idea that a shear flow is the driving force behind the formation and kinematics of MBM 40. There is a continuous flow of atomic gas through the region, encompassing the molecular cloud. Additionally, a large quantity of H I exists on the eastern and northern sides of the maps at velocity ~1 km s^{-1}, and another in the west and southwest at ~5 km s^{-1}. In between these velocities is both the molecular gas comprising MBM 40 and the atomic H I shell clearly visible in channels 1006 – 1016. Taken together, the atomic and molecular data suggest the presence of a flow through the

region from the northeast to the southwest. If this were indeed a shear flow, it could both provide continuously energy injection into the molecular cloud, thus keeping it from collapsing, and it could account for the formation of the cloud itself, as described above. In more detail, the shear flow sets up density gradients at the boundary with the non-flowing, ambient gas. At this point, the denser regions produce a temperature drop within their boundaries (because dense regions cool faster than less dense regions). The temperature drop causes greater condensation, which causes greater cooling, and a runaway effect is created. This runaway is called a thermal instability and for it to work, it needs a trigger. In this case, the trigger is clearly the shear flow. As the H I collects in ever cooler, denser areas, it cools further until eventually molecules form. Since a shear flow constantly injects energy into the cloud, the molecular hydrogen and H I would remain turbulent. This explains why no star formation is seen within MBM 40, even though MBM 40 has dense enough regions as to be close to gravitationally bound. Thus, in summary, shear flows can account for the creation, structure, and behavior of MBM 40 and they are consistent with the H I data presented in this thesis.

5.3 Final Thoughts

In this thesis I presented H I data obtained from the Arecibo radio telescope in a region at high Galactic latitudes containing an interstellar molecular cloud named MBM 40. By examining the H I and the molecular data together, a coherent picture of the interstellar gas in this region was obtained. The data are consistent with the presence of a turbulent mechanism, the shear flow, which can produce dense structures in low density gas. The shear flow mechanism produces both dense structures from the gas which then

become molecular and also keeps the newly-formed molecular cloud from collapsing. This picture works well for the case of MBM 40, but the data described here are relatively low resolution (~4 arcminutes for the H I). The molecular data are at an angular resolution of 45 arcseconds and at a velocity resolution of 0.06 km/s. A more thorough analysis using data with both higher spatial and also higher velocity resolution would definitely rule in favor for or against the shear flow model. Unfortunately, higher spatial resolution data in H I would require an interferometer rather than a single dish (there is no single dish larger than Arecibo in the world). This type of observation requires very different analysis techniques than the ones presented in this thesis, though it would be the necessary next step. Until the H I data can better match the molecular data, the study presented here is typical of the best that can be done when trying to examine the relationship between the atomic and molecular interstellar medium.

Appendix A

There are many different types of celestial coordinates depending upon which what objects you wish to discuss. The two most common ones (and the only two used in this thesis) are equatorial coordinates and galactic coordinates.

Equatorial coordinates are the traditional astronomical system based on the Earth's latitude and longitude. By projecting the Earth's longitude into the sky, we get the meridians of celestial longitude; however, they are called right ascension and are often measured in hours, minutes, and seconds of time. One hour in right ascension equals 15 (so that 24 hours = 260, one minute of right ascension equals a quarter of a degree, or 15 arcminutes, and so on). Celestial latitude is a projection of the latitude system onto the celestial sphere and, in this case, the celestial coordinate is called declination. Like latitude, declination runs from 0 at the celestial equator to 90 at the North Celestial Pole, and -90 at the South Celestial Pole. (Refer to Figure A.1)

Equatorial coordinates are excellent for locating stars on the celestial sphere, but they are clearly based on the Earth, and the Earth has no preferential orientation with respect to the Galaxy. Thus, Galactic coordinates (*l* for Galactic longitude and *b* for Galactic latitude) have to be defined.

If the Galaxy is modeled as a thin pancake, viewed from above, galactic longitude is defined as shown in Figure A.1. The longitude is described with a side view of the pancake (Figure A.2).

The relationship between Right Ascension and declination with *l* and *b* is given by:

$$\cos b \cos(l - 33°) = \cos\delta \cos(\alpha - 282.25°)$$
$$\cos b \sin(l - 33°) = \sin\delta \sin 62.6° + \cos\delta \sin(\alpha - 282.25°) \cos 62.6°$$
$$\sin b = \sin\delta \cos 62.6° - \cos\delta \sin(\alpha - 282.25°) \sin 62.6°$$

Figures for Appendix A

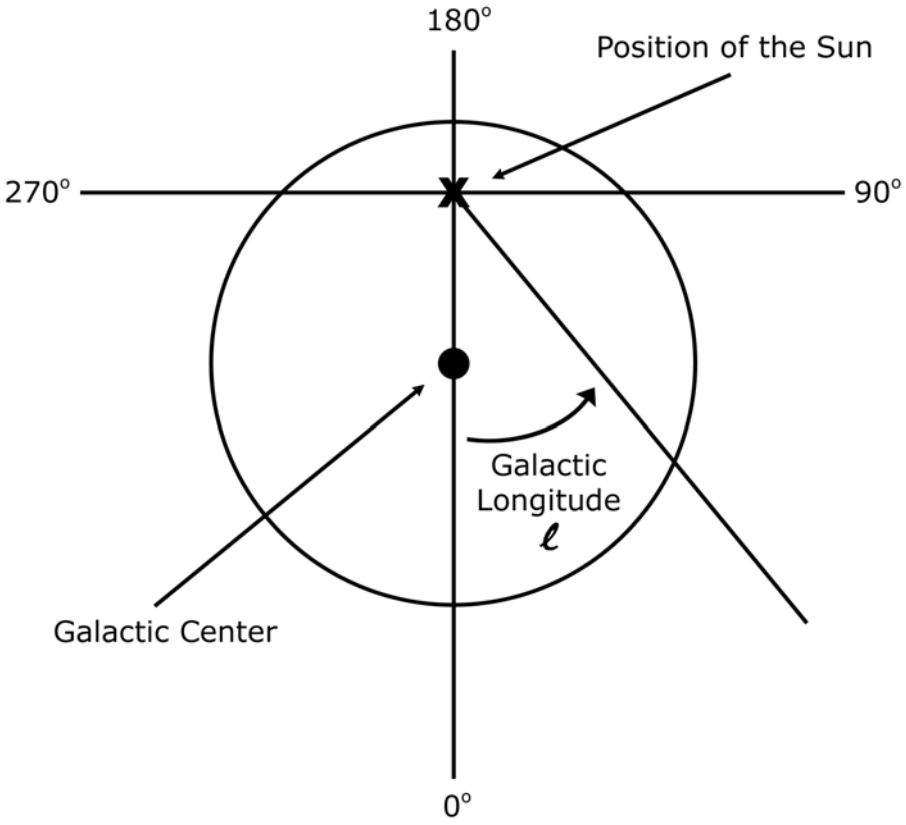

Figure A.1 Galactic Longitude

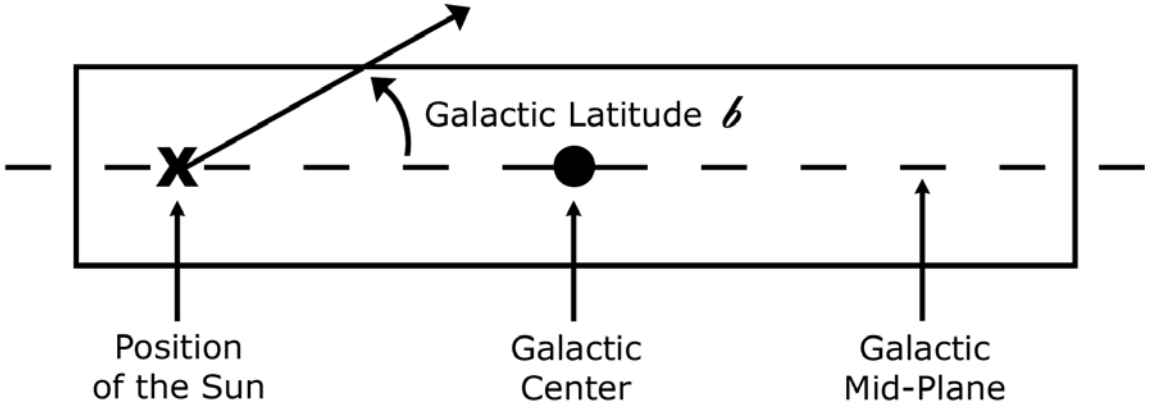

Figure A.2 Galactic Latitude

References

Barnard, E.E. 1927, Photographic Atlas of Selected Regions of the Milky Way, eds. E. B. Frost & M. R. Calvert, (Washington: Carnegie Institution of Washington)

Bhatt, H. C. 2000, A&A, 362, 715

Blitz, L. 1978, Ph. D. Thesis, Columbia University

Blitz, L., Fich, M., & Stark, A. A. 1982, ApJS, 49, 183

Burton, W. B. & Gordon, M. A. 1978, A&A, 63, 7

Colomb, F. R., Pöppel, W. G. L., & Heiles, C. 1980, A&AS, 40, 47

Dame, T. M. 1984, Ph.D. Thesis, Columbia University

Dame, T.M., Hartmann, D., & Thaddeus, P. 2001, ApJ, 547, 792

de Vries, H. W. 1988, Ph. D. Thesis, Columbia University

Dickey, J. M. & Lockman, F. J. 1990, ARA&A, 28, 215

Ewen, M. I. & Purcell, E. M.1951, Nature, 168, 356.

Gir, B. Y., Blitz, L., & Magnani, L. 1994 ApJ, 434, 162

Hearty, T. 1998, Ph. D. Thesis, University of Georgia

Heiles, C. et al. 2000, Arecibo Technical Memo 2000-04

Low, F. J. et al. 1984, ApJ, 278, 219

Lynds, B. T. 1962, ApJS, 7, 1

Magnani, L., Blitz, L., & Mundy 1985, ApJ, 295, 402

Magnani, L., Hartmann, D., & Speck, B. G. 1996, ApJ, 465, 825

Muller, C. A. & Oort, J. H.1951, Nature, 168, 357

Myers, P.C. 1985, in Protostars and Planets II, ed. D. C. Black & M. S. Matthews (Tuscon: U of Arizona), 81

Penprase B. E. 1993, ApJS, 88, 433

Sanders, D. B., Solomon, P. M., & Scoville, N. Z. 1984, ApJ, 276, 182

Shore, S. N., Magnani, L., LaRosa, T. N., & McCarthy, M. N. 2003, ApJ, in press

Spitzer, L. Jr., 1978, *Physical Processes in the Interstellar Medium*, (New York: John Wiley and Sons)

Stark, A.A. 1979, Ph.D. Thesis, Princeton University

van Dishoeck, E. F. & Black, J. H. 1988, ApJ, 334, 771

van Dishoeck, E. F., Phillips, T. G., Black, J. H., & Gredel, R. 1991, ApJ, 366, 141

Verschurr, G. L. 1974, ApJS, 27, 283

Welty, D. E., Hobbs, L. M., Blitz, L., & Penprase, D. E. 1984, ApJ, 346, 232

Wilson, R. W., Jefferts, K. B., Penzias, A. A. 1970, ApJ, 161, 243